

sumed no changes in the magnitude of the interaction strengths for the surface spins. The surface spin wave obtained in Ref. 7 splits off from the bulk spectrum from *below*, in contrast to the surface spin wave in the itinerant-electron model, which always lies *above* the bulk-spin-wave spectrum (even at $q_{\parallel} = 0$).

It is clear that surface spin waves in itinerant-electron ferromagnets generally involve relatively high frequencies. Their study by microwave ferromagnetic resonance techniques would only be possible for small values of the exchange splitting. We have seen that in strong ferromagnets, the long-wavelength surface modes are highly localized near the surfaces and thus an ideal probe would be by spin-polarized electron scattering or energy-loss measurements. Indeed, in such experiments, the large energies of long-wavelength itinerant surface spin waves will be an advantage in removing energy resolution difficulties. More indirectly, the existence of these modes may show up by their effect on the rate of chemical reactions on ferromagnetic metal sur-

faces.⁸

*Work supported by the National Research Council of Canada.

¹For a review, see D. L. Mills, J. Phys. (Paris), Colloq. **31**, C1-33 (1970).

²E. Zaremba and A. Griffin, Can. J. Phys. **53**, 891 (1975).

³See, for example, H. Yamada and M. Shimizu, J. Phys. Soc. Jpn. **22**, 1404 (1967); R. D. Lowde and C. G. Windsor, Adv. Phys. **19**, 813 (1970); J. F. Cooke, Phys. Rev. B **7**, 1108 (1973).

⁴G. Gumbs and A. Griffin, to be published.

⁵We remark that in the complete absence of a finite-range interaction [i.e., $I(\vec{q}) = I_0$], one can show (see Ref. 2) that the poles of χ_{+-} for a slab are given by the zeros of $\epsilon_M(q_{\parallel}, q_z, \omega)$, rather than the zeros of D defined in (9). The only way the boundaries come in in this case is to restrict the values of q_z to multiples of π/L , corresponding to bulk-mode standing waves.

⁶S. C. Ying, L. M. Kahn, and M. T. Beal-Monod, Solid State Commun. **18**, 359 (1976).

⁷R. F. Wallis, A. A. Maradudin, I. P. Ipatova, and A. A. Klochikhin, Solid State Commun. **5**, 89 (1967).

⁸See, for example, K. G. Petzinger and D. J. Scalapino, Phys. Rev. B **8**, 266 (1973).

Direct Study of the Nature of Nitrogen Bound States in GaAs_{1-x}P_x:N[†]

George G. Kleiman

Instituto de Física, Universidad Nacional Autónoma de México, México 20, Distrito Federal, México

and

R. J. Nelson, N. Holonyak, Jr., and J. J. Coleman

Department of Electrical Engineering and Materials Research Laboratory, University of Illinois at Urbana-Champaign, Urbana, Illinois 61801

(Received 11 May 1976)

A new theory in which the observed electronic states in N-doped GaAs_{1-x}P_x derive from the *combination* of a *long-range* disorder and strain-induced nitrogen-associated potential and the usual *short-range* isoelectronic nitrogen potential is compared with pressure measurements at $x \sim 0.30$ (and with earlier measurements at $x \gtrsim 0.45$). In the composition region $x \sim 0.3$ a strong N_T-N_X interaction is predicted and is observed by pressure measurements.

Recent experimental studies of nitrogen-doped In_{1-x}Ga_xP¹ and GaAs_{1-x}P_x²⁻⁴ lead to a new interpretation of the previously observed⁵ N-trap luminescence transitions in these materials. The broad luminescence band previously attributed to NN pairs arises from recombination between holes and electrons in single nitrogen bound states (labeled N_X) with a strong phonon sideband.¹⁻³ In addition, the transitions identified in early work as NN₃ pairs ($x = 0.37, 0.38$)^{5,6} and the A line ($0.40 \leq x \leq 0.53$)^{5,7} in GaAs_{1-x}P_x:N are

actually an additional N-trap bound state (N_T)^{2,4} with a smaller binding energy than N_X. Hydrostatic-pressure experiments, in which the Γ and X energy gaps change with pressure and allow the *continuous* study of these states over a simulated composition range, demonstrate that the deep N_X state is derived primarily from the X-conduction-band minima for $x \gtrsim 0.42$ ² and that the shallow bound state, N_T, follows the Γ minimum for $0.30 \leq x \leq 0.45$ and then bends and follows X for $0.45 \leq x \leq 0.53$. In this latter range, as the present

work indicates, the N-trap state is due to the short-range potential commonly attributed to the N impurity. These experimental observations²⁻⁴ in GaAs_{1-x}P_x:N are in quantitative agreement with predictions of a new theory⁸ in which the observed electronic states derive from the combination of a long-range disorder and strain-induced nitrogen-associated potential, V_l , which by itself induces one state (n_Γ , energy W_{n_Γ}) associated with Γ and one (n_x , energy W_{n_x}) with X, and the usual⁵ short-range isoelectronic nitrogen potential, V_s , which induces a state (n , energy W_n) delocalized in momentum. These are illustrated schematically in Fig. 1(a). This theory,⁸ therefore, provides a totally different picture of the relevant physical mechanisms from that of previous work.^{9,10}

One of the consequences of this theory is that the eigenstates corresponding to $V_l + V_s$ [which are denoted by N_Γ' , N_Γ , and N_X in order of decreasing energy, as displayed in Fig. 1(b)] contain ad-

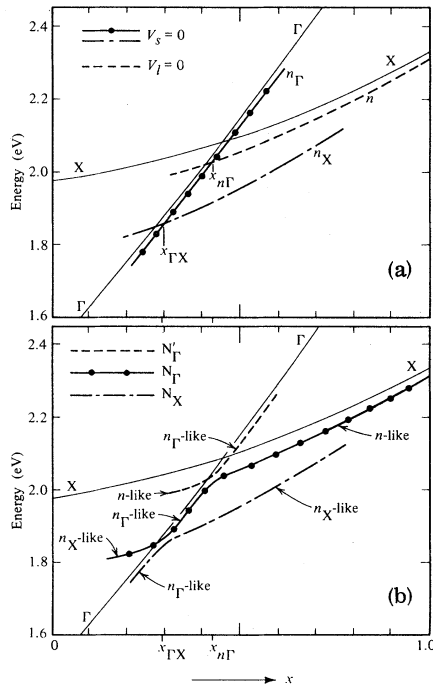


FIG. 1. (a) Schematic illustration of composition dependence of bound-state energies produced by the long-range (V_l) and short-range (V_s) nitrogen potentials before they are combined. The compositions x_{n_Γ} and $x_{\Gamma X}$ correspond, respectively, to $W_n = W_{n_\Gamma}$ and $W_{n_\Gamma} = W_{n_x}$. We neglect the small Γ -X hybridization at $x = x_{\Gamma X}$. (b) Corresponding diagram for bound states produced by combining V_l and V_s (i.e., $V_l \neq 0$ and $V_s \neq 0$). The splitting near x_{n_Γ} and $x_{\Gamma X}$ is illustrated. As $x \rightarrow x_{\Gamma X}$, the energy of N_X is pushed down by n_Γ , which it approaches. In this region, the energy of N_Γ approaches that of n_x . These points are discussed in the text.

mixtures of the n , n_Γ , and n_x states. There is strong splitting of the energies in the regions where $W_n \sim W_{n_\Gamma}$ (i.e., $x \sim x_{n_\Gamma}$) and $W_{n_\Gamma} \sim W_{n_x}$ (i.e., $x \sim x_{\Gamma X}$), as shown in Fig. 1. In particular, for $x \sim x_{\Gamma X}$, the energies of both N_Γ (E_{N_Γ}) and N_X (E_{N_X}) are predicted to vary strongly with pressure, in contrast to the behavior of states derived from the X minima alone.² While the pressure behavior of N_Γ and N_X has been studied in the composition region $x \gtrsim 0.38$ where they are well separated in energy and where N_Γ changes character ($x \gtrsim 0.45$),² it is of fundamental interest to examine their behavior at still lower compositions, where they approach one another and interact, in order to provide a further test of the physical picture of the theory. We describe here the application of this theory to explain the behavior of the N trap in the region ($x \sim 0.3$) where the N_Γ - N_X interaction is strong. Pressure data are presented exhibiting the behavior predicted by theory, i.e., N_Γ - N_X interaction and the resulting splitting of these two states, which are themselves a consequence of the long-range potential, V_l .⁸ From these results and the general agreement of theory and experiment,^{2-4,8} we conclude that the physical picture presented by the theory is a faithful model of the processes operative in the GaAs_{1-x}P_x:N alloy system. Possible origins of V_l relating to strain and disorder are discussed elsewhere.⁸

We represent V_s by the one-band one-site Koster-Slater approximation,¹¹ as in previous theoretical work,^{9,12,13} and denote its matrix element between Wannier states by V_0 ; we assume that the nitrogen is located at the site $R_0 = 0$. The energy eigenvalues, E_j (i.e., $j = N_X, N_\Gamma$, and N_Γ'), corresponding to the combined potential $V_l + V_s$ (which we assume to couple only to the lowest-energy conduction band, denoted by index c) are given by solutions of

$$\text{Re}[G(\vec{R}_0, \vec{R}_0, E)] = 1/V_0. \quad (1)$$

G is the retarded conduction-band Green's function corresponding to V_l in the Wannier representation and obeys the following equations:

$$G(\vec{R}_m, \vec{R}_s, E) = \sum_{k=\Gamma, X} \frac{f_{n_k}(\vec{R}_m) f_{n_k}^*(\vec{R}_s)}{E - W_{n_k} + i\delta} + G_c(\vec{R}_m, \vec{R}_s, E), \quad (2a)$$

$$[E_c(\hbar\nabla/i) + V_l(\vec{r}) - W_k] f_k(\vec{r}) = 0. \quad (2b)$$

G_c , E_c , and δ denote, respectively, the continuum portion of G , the conduction-band dispersion relation, and 0^+ . Equation (2b) follows from the long-

range nature of V_i , and the bound states n_Γ and n_x are localized in momentum about their respective minima. Deep in the gap, $G_c \cong \Lambda$, the value of G when $V_i=0$. For simplicity, we let $G_c \cong \Lambda$ throughout the bound-state region and neglect the effect of V_i on continuum states; its long-range nature makes this reasonable.

We are interested in the region where $W_{n_x} \simeq W_{n_\Gamma} \ll W_n$. [Note that on the line W_m , $V_0\Lambda(W_n)=1$; also we ignore the relatively small hybridization of W_{n_x} and W_{n_Γ} here.] Because $V_0\Lambda < 1$ here, the antisymmetric divergent n_Γ and n_x bound-state terms resulting from inserting Eq. (2a) into Eq. (1) make $E_{N_\Gamma} < \max(W_{n_\Gamma}, W_{n_x})$ and $E_{N_x} < \min(W_{n_\Gamma}, W_{n_x})$. In particular for $x > x_{\Gamma X}$, as $W_{n_\Gamma} \rightarrow W_{n_x}$, n_Γ pushes E_{N_x} increasingly below W_{n_x} (the quantity $x_{\Gamma X}$ denotes the composition where $W_{n_\Gamma} = W_{n_x} \equiv W_{\Gamma X}$). As W_{n_Γ} decreases, this process continues until, eventually, E_{N_x} is determined by W_{n_Γ} alone. On the other hand, as $W_{n_\Gamma} \rightarrow W_{\Gamma X}$ from above, $E_{N_\Gamma} \rightarrow W_{\Gamma X}$. As W_{n_Γ} decreases further, $W_{n_x} > E_{N_\Gamma} > W_{n_\Gamma}$, and the influence of n_Γ decreases until E_{N_Γ} is determined by W_{n_x} alone (E_{N_Γ} is resonant in this region). The energies E_{N_Γ} and E_{N_x} are displayed in Fig. 1(b), where we indicate the regions where the eigenvalues are determined primarily by one of the n states by the term n -like.

The preceding discussion reflects the general consequences of the physical model without recourse to specific models. It is clear that both E_{N_Γ} and E_{N_x} should be sensitive to pressure for $x \sim x_{\Gamma X}$.

The corresponding $\vec{k}=0$ momentum amplitudes, A_{N_j} (i.e., $j = \Gamma, X$), which yield a measure of the oscillator strengths, are given by

$$A_{N_j} \cong \left[\frac{C_{n_\Gamma} f_{n_\Gamma}(0)}{E_{N_j} - W_{n_\Gamma}} + \frac{1}{E_{N_j} - E_\Gamma} \right] \times [-G'(0, 0, E_{N_j})]^{-1/2}, \quad (3a)$$

$$C_{n_\Gamma} \equiv \sum_{\vec{R}_m} \vec{r}_m f_{n_\Gamma}(\vec{R}_m). \quad (3b)$$

In Eq. (3a), $G'(E) \equiv dG(E)/dE$, $E_\Gamma \equiv E_c(\vec{k}=0)$, and C_{n_Γ} is the strong $\vec{k}=0$ amplitude of n_Γ . We have neglected the small $\vec{k}=0$ amplitude of n_x and chosen f_{n_Γ} to be real. From our discussion, we can understand the x dependence of A_{N_x} . As x decreases, $E_{N_x} \rightarrow W_{n_\Gamma}$ and the strong C_{n_Γ} amplitude makes an increasing contribution. The second term in Eq. (3a) corresponds to the usual band-structure-enhancement (BSE)⁵ term whose magnitude at first increases and then levels off as E_{N_x} tends to become parallel to W_{n_Γ} as shown in Fig. 1(b). These two terms have the same sign

and reinforce each other so that $|A_{N_x}|$ increases as $x \rightarrow x_{\Gamma X}$ from above. In A_{N_Γ} , on the other hand, $E_{N_\Gamma} - W_{n_\Gamma}$ increases as x decreases below $x_{\Gamma X}$ so that C_{n_Γ} makes a decreasing contribution. At the same time $E_{N_\Gamma} \rightarrow E_\Gamma$ and the magnitude of the BSE term increases. These terms have opposite signs so that there is a point at which $|A_{N_\Gamma}|=0$ after which the BSE term is dominant.

For the pressure measurements of this work, N-doped GaAs_{1-x}P_x substrates¹⁴ are prepared into In_{1-y}Ga_yP_{1-z}As_z-GaAs_{1-x}P_x:N single heterojunctions¹⁵ that do not absorb the higher-energy side of the electroluminescence spectrum, which is important in the region where near-band-edge emission is observed. A helium-gas pressure system¹⁶ and a pressure vessel with a sapphire optical window¹⁷ are used for the measurements. The pressure vessel is submerged in a liquid-nitrogen bath. Fiber optics are used to collect the diode luminescence and to direct the light into a 0.5-m grating monochromator. A Manganin gauge is used for pressure measurements. The pressure coefficients of the Γ and X energy gaps of GaAs_{1-x}P_x are known from previous work^{2,18} to be $dE_\Gamma/dp \sim 10^{-5}$ eV/bar and $dE_X/dp \sim -10^{-6}$ eV/bar. The combined pressure variation of the band gaps simulates a composition change of $dx/dp \sim 1.1\%/kbar$.

Figure 2 shows the electroluminescence spectra of $x=0.32$ GaAs_{1-x}P_x:N at 77°K. At 0 kbar and a current density of 80 A/cm², curve *a* shows the peak of the N_x transition at ~ 6765 Å and a high-energy shoulder at ~ 6700 Å corresponding to near-band-edge emission (Γ) with some contribution from the shallow N_Γ state. The 6.3-kbar spectrum (corresponding to $x \approx 0.39$) of curve *b* demonstrates the ~ 58 -meV pressure shift expected of the Γ - N_Γ transitions.^{2,19} The observed 37-meV shift of the N_x transition is *in direct contrast* with the negligible pressure shift observed previously for N_x at compositions $x \geq 0.42$, N_Γ and N_x are well separated in energy, and the pressure coefficient of N_x is similar to that of the indirect gap (i.e., $dE_X/dp \sim -1$ meV/kbar). The large shift observed for N_x at $x=0.32$ in Fig. 2 is expected [cf. Fig. 1(b)] because of the strong interaction and shift of N_Γ with pressure away from N_x states in this composition range.

The inset of Fig. 2 shows also the N_x intensity, at constant current density, as a function of pressure. The observed decrease in intensity, which reflects a decreasing oscillator strength or $\vec{k}=0$ component of the N_x wave function as Γ - N_Γ re-

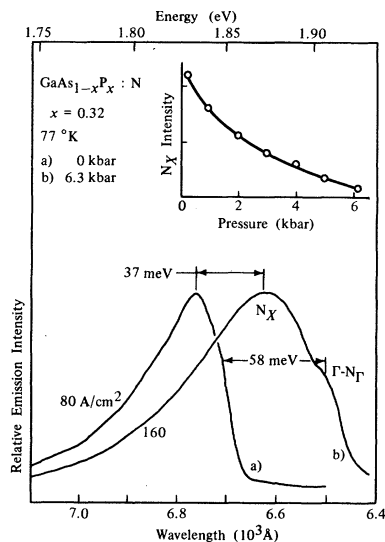


FIG. 2. Pressure variation of electroluminescence spectrum for $\text{GaAs}_{0.68}\text{P}_{0.32}:\text{N}$ showing the pressure sensitivity of N_X and N_Γ , which reflects the strong admixture of the states, in agreement with theoretical predictions. This is in contrast to the pressure insensitivity of N_X at higher compositions, where the influence of N_Γ is negligible. The inset displays the decrease of N_X intensity with increasing pressure (increasing simulated composition), reflecting the decreasing admixture of N_Γ .

cedes, is a consequence of the interaction between the N_Γ and N_X states and the resultant mixing of the wave functions.¹⁹ That is, at reduced pressure ($\Gamma-N_\Gamma$ closer to N_X), the $N_\Gamma-N_X$ interaction is strong and depresses the position (energy) of the N_X state. Also, the increasing proximity of the Γ band edge increases the N_X oscillator strength. It is clear from experiment and theory that in the crystal composition region $x \sim 0.3$ the $N_\Gamma-N_X$ interaction causes the long-range N_X state to be displaced downward.

The results of this study serve to explain the general behavior of the N_Γ and N_X states in the region $x \sim 0.3$. The physical picture of a combined short-range-long-range nitrogen potential independent of specific models for N-doped $\text{GaAs}_{1-x}\text{P}_x$ is consistent with experimental data at $x \sim 0.3$ and at $x \geq 0.45$.² This picture is in contrast to previous work^{5,10,12,13,20} employing the idea of only a single potential.

We are grateful to M. G. Craford, W. O. Groves, D. L. Keune, and D. Lazarus for their help in this work, and to Yuri S. Moroz, R. Gladin, K. Kuehl, B. Marshall, and M. Runyon for technical assistance.

†This work has been supported in part by the National Science Foundation, Grant No. DMR-72-03045-A01, and by the Advanced Research Projects Administration, U. S. Department of Defense, monitored by the U. S. Air Force Office of Scientific Research under Contract No. F44620-75C-0091.

¹R. J. Nelson and N. Holonyak, Jr., *J. Phys. Chem. Solids* **37**, 629 (1976).

²R. J. Nelson, N. Holonyak, Jr., J. J. Coleman, D. Lazarus, W. O. Groves, D. L. Keune, M. G. Craford, D. J. Wolford, and B. G. Streetman, *Phys. Rev. B* **14**, 685 (1976).

³D. J. Wolford, B. G. Streetman, R. J. Nelson, and N. Holonyak, Jr., to be published.

⁴D. J. Wolford, B. G. Streetman, W. Y. Hsu, J. D. Dow, R. J. Nelson, and N. Holonyak, Jr., *Phys. Rev. Lett.* **36**, 1400 (1976).

⁵M. G. Craford and N. Holonyak, Jr., in *Optical Properties of Solids: New Developments*, edited by B. O. Seraphin (North-Holland, Amsterdam, 1975), Chap. 5.

⁶R. D. Dupuis, N. Holonyak, Jr., M. G. Craford, D. Finn, and W. O. Groves, *Solid State Commun.* **12**, 489 (1973).

⁷N. Holonyak, Jr., R. D. Dupuis, H. M. Macksey, M. G. Craford, and W. O. Groves, *J. Appl. Phys.* **43**, 4148 (1972).

⁸George G. Kleiman, unpublished.

⁹See Ref. 5 for appropriate citations of previous theoretical work.

¹⁰A previous theoretical treatment (in Ref. 4) describes both N_Γ and N_X in the direct region as arising from a single short-range potential, which causes the states to have high $k=0$ components. In order to explain the experimental association of N_Γ with Γ and N_X with X , however, these states are assumed to obey the effective-mass approximation near their respective minima. This assumption is inconsistent with the nature of short-range potentials, which involve the conduction-band energy over *all* momenta, so that *both* states would follow either Γ or X if they arose from a short-range potential.

¹¹G. F. Koster and J. C. Slater, *Phys. Rev.* **95**, 1167 (1954).

¹²R. A. Faulkner, *Phys. Rev.* **175**, 991 (1968).

¹³D. R. Scifres, N. Holonyak, Jr., C. B. Duke, G. G. Kleiman, A. B. Kunz, M. G. Craford, W. O. Groves, and A. H. Herzog, *Phys. Rev. Lett.* **27**, 191 (1971).

¹⁴M. G. Craford and W. O. Groves, *Proc. IEEE* **61**, 862 (1973).

¹⁵J. J. Coleman, W. R. Hitchens, N. Holonyak, Jr., M. J. Ludowise, W. O. Groves, and D. L. Keune, *Appl. Phys. Lett.* **25**, 725 (1974).

¹⁶J. D. Weiss and D. Lazarus, *Phys. Rev. B* **10**, 456 (1974).

¹⁷D. B. Fitchen, *Rev. Sci. Instrum.* **34**, 673 (1963).

¹⁸T. A. Fulton, D. B. Fitchen, and G. E. Fenner, *Appl. Phys. Lett.* **4**, 9 (1964).

¹⁹This pressure behavior is similar to that observed (Ref. 2) near $x \sim 0.5$ which is a result of similar fundamental mechanisms.

²⁰George G. Kleiman, *J. Appl. Phys.* **47**, 180 (1976).